MHD-CHANNEL FLOW OF LIQUID METAL UNDER AN INHOMOGENEOUS MAGNETIC FIELD. PART 2: DIRECT NUMERICAL SIMULATION

E. V. Votyakov, E. Zienicke, A. Thess

Fakultaet fuer Maschinenbau, Technische Universitaet Ilmenau, PF 100565, 98684 Ilmenau, Germany (Evgeny.Votyakov@TU-Ilmenau.de)

Introduction. We studied numerically a liquid metal flow under an inhomogeneous magnetic field in a rectangular channel. The freeware parallel 3D flow solver NaSt3DGP (created in the group of Prof.Griebel) was used as a basement to develop our MHD solver for a quasistatic approximation.

The main phenomenon observed in the simulation is the appearance of a M-shape profile for streamwise velocity under the magnet. We have compared our simulation with the experimental data (see *MHD-Channel Flow ... Part 1*, and [1]) and found good agreement for the electric field distribution and the mean streamwise velocity profile. As well, our results support the existence of two large-scale vortices under the magnets that is indirectly implied by the experimentally found distribution of the electric potential. To describe quantitatively an experimentally found suppression of the velocity fluctuations, the further simulation requires a finer grid resolution.

1. Equations, Algorithm, Solver. We apply the inductionless approximation, where the governing equations for an electrically conducting and incompressible fluid are (all values are dimensionless):

$$\frac{\partial \mathbf{v}}{\partial t} + (\mathbf{v}\cdot\nabla)\mathbf{v} = -\nabla p + \frac{1}{\mathrm{Re}}\triangle\mathbf{v} + \frac{\mathrm{Ha}^2}{\mathrm{Re}}(\mathbf{j}\times\mathbf{B}), \quad (1)$$

$$\nabla\cdot\mathbf{v} = 0, \quad (2)$$

$$\mathbf{j} = -\nabla\phi + \mathbf{v}\times\mathbf{B}, \quad (3)$$

$$\triangle\phi = \nabla\cdot(\mathbf{v}\times\mathbf{B}). \quad (4)$$

These equations are derived from the full MHD system with the assumption that an induced magnetic field is infinitely small in comparison to the external magnetic field (see, e.g., [2, 3]).

As a base for our solver, we have selected NaSt3DGP - the simulation code of the working group of Prof. Griebel (see [4]). Originally, this finite-difference solver was designed for pure hydrodynamical problems. Therefore, we had to extend it by the following features to be able to solve MHD problems: (1) using the Poisson solver also for the determination of the electric potential, and (2) inserting the Lorentz force contribution into a preliminary velocity field. Moreover, we reorganized the input and output parts of NaSt3DGP in order to work with the arrays keeping the magnetic field, the electric potential, and the electric current.

All the results presented below were obtained for a rectangular channel ($50 \times 10 \times 2$, so the aspect ratio is $25 : 5 : 1$) and resolution ($128 \times 90 \times 64$) on an inhomogeneous grid. This corresponds to the aspect ratio of the measuring volume in the experiments. The resolution is sufficiently fine first to reach a steady state flow in a reasonable time and second to see the large scale peculiarities of the flow. However, the selected resolution is not good enough to study quantitatively the

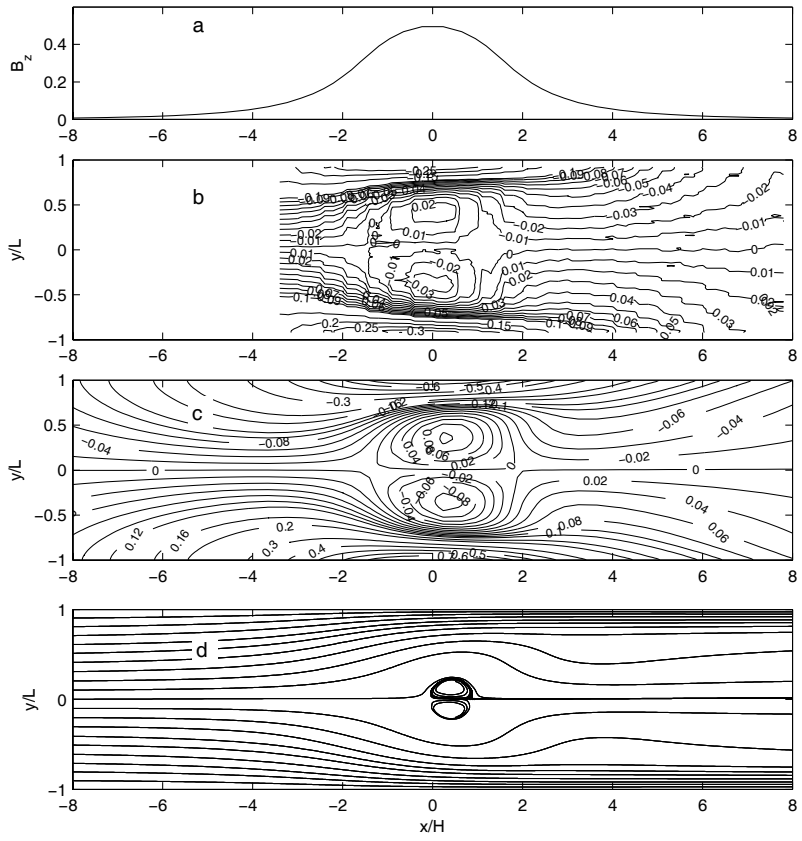

Fig. 1. Strength of the magnetic field (a), experimentally measured (b) and numerically simulated (c) contour plots for the electric potential, and streamlines projection (d). All results are for a steady-state flow at the half height of the channel, $z = 0$, Re $= 4000$, Ha $= 400$, resolution $128 \times 90 \times 64$.

fluctuations of the turbulent flow. Therefore, we will not compare the numerical and experimental results for velocity fluctuations. The magnetic field configuration used for the simulations was obtained by magnetic field measurements on the experimental setup. Besides the geometry, the two principal parameters for the simulations are the Reynolds and the Hartmann numbers. They are chosen to be the same as in experiments: Re $= 4000$, Ha $= 400$.

2. Results of simulation. Fig. 1 gives a comparison for the electric potential in a steady-state flow at the half height of the channel. It consists of four parts having the same scale for the x-axis which is in the streamwise direction. The upper part (Fig. 1a) is an intensity profile for the magnetic field along the channel. Then, there are two contour plots composed of the electric potential lines, experimentally measured (Fig. 1b) and numerically simulated (Fig. 1c). The last part, obtained from the simulation, gives the projection of streamlines (which coincide with the particle paths in a steady-state flow) onto the horizontal plane in the center of the channel (Fig. 1d).

The two contour plots for the electric potential (Fig. 1b, c) demonstrate a qualitative agreement between the experimental and numerical results. In particular, the main features are closed lines in the part, where the strength of the magnetic field is maximal. One can see that these closed loops are present both in the

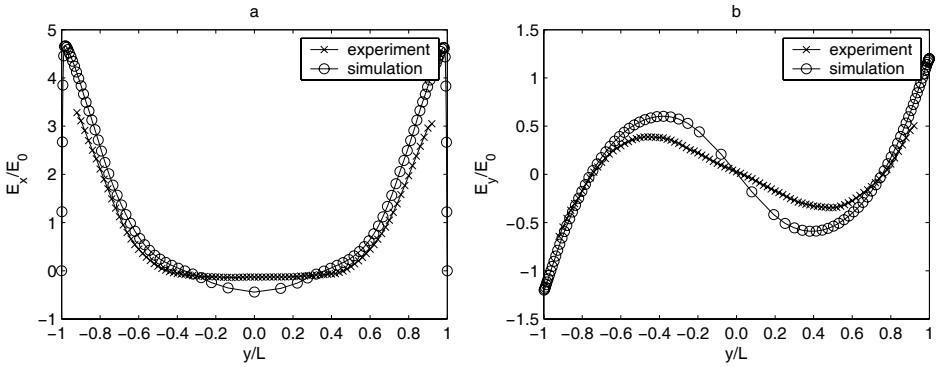

Fig. 2. Numerically simulated (circles) and experimentally measured (crosses) of longitudinal (a) and transverse (b) electric fields, $x/H = 0.5$.

experimental and numerical plots.

What is the meaning of the above mentioned closed lines of the electric potential? As an example, let us consider a metallic cylinder and start to rotate this cylinder in an external magnetic field. It can be shown that this rotation will form the closed lines of the electric potential around the cylinder. By analogy, we can suggest that the observed concentric closed lines of the electric potential, found both experimentally and numerically, are due to large-scale vortices forming in the flow under the magnet. To check this hypothesis, we have calculated particle paths in the center of the channel and actually found these two vortices, see Fig. 1*d*. Thus, the presented numerical simulation supplements the experimental results.

A more detailed comparison between the numerically simulated and experimentally measured strength of the electric field one can see in Fig. 2. The longitudinal electric field is defined as $E_x = -\partial\phi/\partial x$, and the transverse one – $E_y = -\partial\phi/\partial y$. Since the behavior for the experimental and simulated electric potential ϕ is similar, the curves of the electric field are similar as well; as to the quantitative agreement, the numerical results slightly overestimate the experimental ones in the region close to the side walls.

So far, our comparison of the numerical and experimental results concerned only the electric potential and quantities that can be derived from the electric potential. The reason is that the electric potential can be measured directly in the experiment (see the paper of Yu. Kolesnikov, O. Andreiev and A.Thess in this Proceedings, and [1]), so it can be compared directly with the simulation. To get the velocity field from the data of the electric potential, one should solve Eq. 4 with the measured ϕ and $\mathbf{B}$. This is very complicated, and it is easier to compare the electric potential data with numerical simulations instead of the velocity field. Outside the magnetic field velocity measurement using *Vives* probes is possible. The stronger the magnetic field, the higher electric potential, and the more precise are experimental data. Inside the magnetic field one cannot measure flow velocities.

Typical M-shape streamwise velocity profiles are illustrated in Fig. 3. There are two cases: close to the magnet ($x/H = 2$, Fig. 3*a*) and further away from the magnet ($x/H = 5$, Fig. 3*b*). Again, one can observe a good accordance between the experimental and numerical curves. It is worth to note that the M-shape profile is well kept even quite far from the magnet. The difference between these two cases (it was shown experimentally [1]) is that the flow far from the magnet initiates a

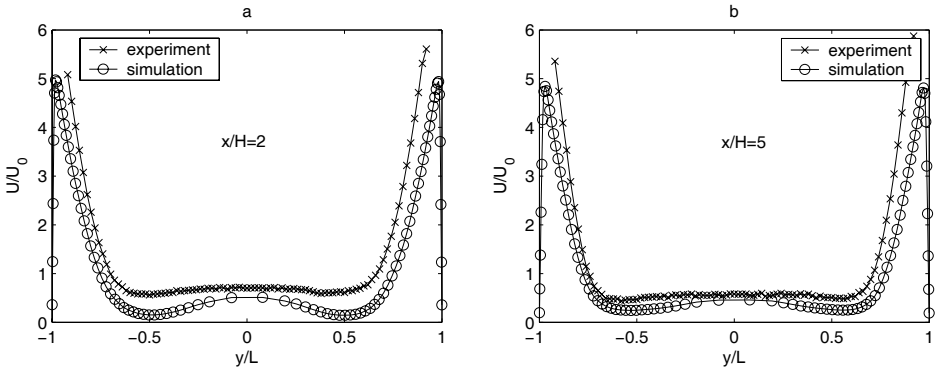

Fig. 3. Numerically simulated (circles) and experimentally measured (crosses) streamwise velocities, $x/H = 2$ (a) and $x/H = 5$ (b).

turbulence, which was suppressed by the magnetic field. The numerical simulation is not able to catch this effect up to now because of insufficient grid resolution.

3. Conclusions. Taking, as a base, NaSt3DGP – the finite-difference computational fluid dynamics solver, we have developed a numerical solver for the magnetohydrodynamic flow with arbitrary configuration of the magnetic field. This solver was verified by the simulation of the liquid metal flow inside a rectangular channel. Results of the simulation were compared with the experimental ones obtained for $\mathrm{Re} = 4000$, $\mathrm{Ha} = 400$. We have found a good agreement for the electric potential distribution and for the streamwise velocity profile. As well, our results verified the existence of two large-scale vortices under the magnets that was indirectly implied by the experimentally found distribution of the electric potential. To describe quantitatively the experimentally found suppression of the velocity fluctuations, further simulation will require a finer grid resolution.

Acknowledgments. The authors express their gratitude to the Deutsche Forschungsgemeinschaft for financial support in the frame of the "Research Group Magnetofluiddynamics" at the Ilmenau University of Technology. The simulations were carried out on a JUMP supercomputer, access to which was provided by the John von Neumann Institute (NIC) at the Forschungszentrum Jülich.

REFERENCES

1. O. Andreiev, Yu. Kolesnikov, A. Thess. Liquid metal flow under inhomogeneous magnetic field. *Phys. Fluids*, (2005) (in press).
2. D. Lee, H. Choi. Magnetohydrodynamic turbulent flow in a channel at low magnetic Reynolds number. *J. Fluid Mech*, vol. 429 (2001), pp. 367–394.
3. D.S. Krasnov, *et al.* Numerical study of instability and transition to turbulence in the Hartmann flow. *J. Fluid Mech*, vol. 504 (2004), pp. 183–211.
4. M. Griebel, T. Dornseifer, T. Neunhoeffer. *Numerische Strömungssimulation in der Strömungsmechanik* (Vieweg Verlag, Braunschweig, 1995).